JOC The Journal of Organic Chemistry

Article

pubs.acs.org/joc

Synthesis and DNA/RNA Binding Properties of Conformationally Constrained Pyrrolidinyl PNA with a Tetrahydrofuran Backbone Deriving from Deoxyribose

Pitchanun Sriwarom, Panuwat Padungros, and Tirayut Vilaivan*

Organic Synthesis Research Unit, Department of Chemistry, Faculty of Science, Chulalongkorn University, Phayathai Road, Patumwan, Bangkok 10330, Thailand

Supporting Information

ABSTRACT: Sugar-derived cyclic β-amino acids are important building blocks for designing of foldamers and other biomimetic structures. We report herein the first synthesis of a C-activated *N*-Fmoc-protected *trans*-(2*S*,3*S*)-3-aminotetrahydrofuran-2-carboxylic acid as a building block for Fmoc solid phase peptide synthesis. Starting from 2-deoxy-D-ribose, the product is obtained in a 6.7% overall yield following an 11-step reaction sequence. The tetrahydrofuran amino acid is used as a building block for a new peptide nucleic acid (PNA), which exhibits excellent DNA binding affinity with high specificity. It also shows preference for binding to DNA over RNA and specifically in the antiparallel orientation. In addition, the presence of the hydrophilic tetrahydrofuran ring in the PNA structure reduces nonspecific interactions and self-aggregation, which is a common problem in PNA due to its hydrophobic nature.

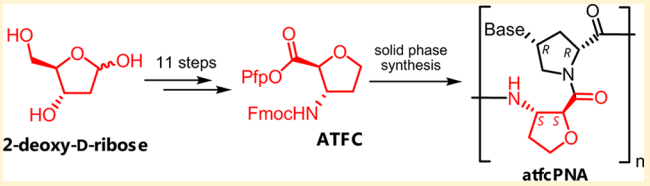

INTRODUCTION

Foldamers are synthetic oligomeric molecules that can mimic naturally occurring biological macromolecules by folding into well-defined secondary structures such as helices, turns, or sheets in solution states.[1] Amino acids, especially cyclic β-amino acids,[2] constitute an important class of building blocks for foldamers.[3] A diverse range of secondary structures were obtained from simple cyclic β-amino acids building blocks with different ring size, stereochemistry, and substituents.[4] The ability to precisely program the folding pattern is not only important from the molecular design aspect but also leads to desirable biological functions. Carbohydrate-derived amino acids[5] have recently attracted much interest as potential building blocks for novel foldamers.[6] It can be readily obtained from inexpensive sources in stereochemically defined configurations and possess a number of functional groups that can be fine-tuned as desired.

Deoxyribonucleoside-derived cyclic β-amino acids have been used in designing nucleobase-containing foldamers,[7] some of which showed promising DNA and RNA binding properties.[7d] These foldamers can therefore be regarded as a new class of peptide nucleic acid (PNA).[8,9] Our research group had introduced a series of conformationally constrained pyrrolidinyl peptide nucleic acids derived from alternating nucleobase-modified D-proline and cyclic β-amino acids.[10,11] A representative member of such pyrrolidinyl PNA is acpcPNA (Scheme 1) which carries *trans*-(1*S*,2*S*)-2-aminocyclopentanecarboxylic acid (ACPC) in the backbone.[10b,d] This acpcPNA showed some distinct properties from DNA and commercial PNA that could be useful for many applications.[12] A recent study on ring homologues suggested that four- or five-membered ring cyclic β-amino acids with specific configurations are essential to provide a balance between rigidity and flexibility that allows the PNA to adopt a DNA-binding conformation.[10e] In addition to ACPC, other five-membered ring heterocyclic β-amino acids had been successfully incorporated into pyrrolidinyl PNA, including 1-aminopyrrolidine-2-carboxylic acid[10a] and 3-aminopyrrolidine-4-carboxylic acid.[10c]

Scheme 1. Structures of acpcPNA and atfcPNA

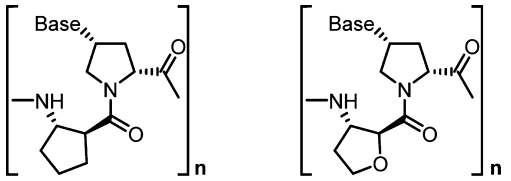

In view of the structural similarity between 3-amino-tetrahydrofuran-2-carboxylic acid (ATFC) and ACPC, it is not surprising that oligomers of ATFC and its ring-substituted derivatives can also form well-defined helical foldamers.[13] Oligomers of *trans*-ATFC formed a 12-helix similar to *trans*-ACPC. On the other hand, the *cis*-isomer adopted a 14-helix structure instead of the extended sheetlike structure of *cis*-ACPC, which was explained based on molecular modeling studies by a more favorable interaction between the less sterically hindered ring of ATFC and the backbone amide group.[13a] We propose that replacement of ACPC in the acpcPNA backbone with *trans*-ATFC should provide a new pyrrolidinyl PNA that can still retain the excellent nucleic acid

Received: April 21, 2015
Published: June 17, 2015

DOI: 10.1021/acs.joc.5b00890
J. Org. Chem. 2015, 80, 7058−7065

Scheme 2. Structural Assignment of Methyl Glycoside Mixture by Conversion into Their 1-Deoxy Perbenzoylated Derivatives

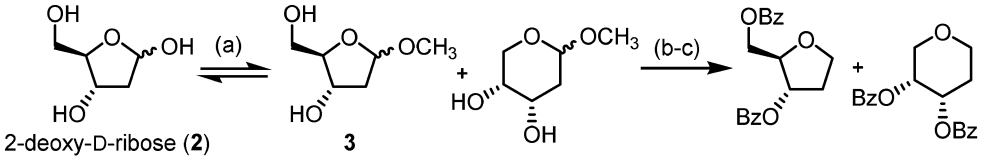

Reaction conditions: (a) methanesulfonic acid, MeOH, time, rt; (b) BzCl, Et_3N, CH_2Cl_2, 0 °C to rt; (c) Et_3SiH, $BF_3{\cdot}OEt_2$, 0 °C to rt

rxn. time	furanose : pyranose
12 h	1.5 : 1
30 min	4 : 1

binding characteristics of acpcPNA. Moreover, it is expected that the more hydrophilic nature of tetrahydrofuran ring in ATFC as opposed to the cyclopentane ring in ACPC should be beneficial in reducing self-aggregation and nonspecific interactions occasionally observed in acpcPNA and other PNA systems due to their uncharged and hydrophobic peptide backbone.[14] Herein, we report the synthesis of a new pyrrolidinyl PNA with an ATFC backbone (will be named atfcPNA, Scheme 1) and a comparison with acpcPNA in terms of DNA/RNA binding properties and nonspecific binding behavior.

RESULTS AND DISCUSSION

Synthesis of Deoxyribose-Derived Cyclic *β*-Amino Acid (*SS*-ATFC). Our previous reports on the effects of stereochemistry of acpcPNA on DNA binding[11] suggests that the appropriately protected (2*S*,3*S*) enantiomer of the *trans*-ATFC (*SS*-ATFC) is required as a key building block. Interestingly, this particular configuration of ATFC is unknown in the literature despite some reports on the remaining stereoisomers.[13a] We proposed that the required *SS*-ATFC monomer **1** should be readily synthesized starting from commercially available 2-deoxy-D-ribose (**2**). The key steps involved reductive removal of the anomeric hydroxyl group, stereospecific introduction of the amino group by a double inversion of configuration at C-3, and oxidation of the C-5 alcohol to the carboxylic acid.

With this synthetic strategy in mind, the anomeric hydroxyl group of 2-deoxy-D-ribose (**2**) was first converted to its methylglycoside derivative in the presence of an acid catalyst (Scheme 2).[15,16] It should be noted that the reaction time played an important role for the outcome of the reaction.[17] ^1H NMR analysis of the product mixture was simplified by perbenzoylation followed by reduction of the anomeric methyl ether with $BF_3{\cdot}Et_2O/Et_3SiH$.[18] Prolonged treatment of **2** with catalytic methanesulfonic acid in MeOH (12 h) provided a 1.5:1 mixture of furanoside **3** and the thermodynamically more stable pyranoside. However, immediate quenching of the reaction after consumption of the starting material (ca. 30 min) afforded the methylfuranoside **3** as the major product (>80% of the crude reaction mixture).

With the optimized conditions in hand, 2-deoxy-D-ribose (**2**) was smoothly converted to methylfuranoside **3** followed by selective protection[19] of the C-5 primary hydroxyl group as the *p*-toluoyl ester to afford furanoside **4** in 67% yield over 2 steps (Scheme 3). Removal of the anomeric methoxy group by treatment with $BF_3{\cdot}Et_2O/Et_3SiH$ was previously reported on a fully protected 2-deoxyribose derivative,[18] and thus it was uncertain if these conditions would be compatible with the unprotected C-3 hydroxyl group of furanoside **4**. It was envisioned that the C-3 hydroxyl group could be "protected" as a sulfonate ester prior to the anomeric reduction. Gratifyingly,

Scheme 3. Synthesis of *SS*-ATFC Starting from 2-Deoxy-D-ribose (2)

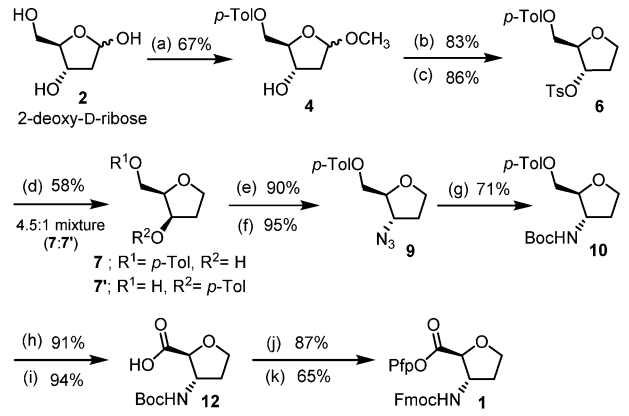

Reaction conditions: (a) i) methanesulfonic acid (cat), MeOH, rt, 30 min, ii) p-toluoyl chloride, pyridine, CH_2Cl_2, 0 °C (b) p-TsCl, DMAP (cat), Et_3N, CH_2Cl_2, 0 °C to rt (c) Et_3SiH, $BF_3{\cdot}OEt_2$, 0 °C to rt (d) $NaNO_2$, DMSO, 120 °C (e) MsCl, DMAP (cat), Et_3N, CH_2Cl_2, 0 °C (f) NaN_3, DMSO, 90-100 °C (g) Pd/C, H_2 (1 atm), Boc_2O, MeOH (h) LiOH, THF:H_2O (1:1), rt (i) TEMPO (cat), BAIB, MeCN:H_2O (1:1), rt (j) i) TFA:CH_2Cl_2 (1:1) ii) FmocOSu, $NaHCO_3$, MeCN:H_2O (1:1), pH 8, rt (k) PfpOTfa, DIEA, CH_2Cl_2

the furanoside **4** was tosylated to afford **5** in 83% yield, and the anomeric methoxy group was successfully reduced to provide intermediate **6** in 86% yield.

We next focused on the nucleophilic displacement of the tosylated furanoside **6**. The nitrite ion ($NaNO_2$) is relatively overlooked as an oxygen nucleophile for the stereochemical inversion of a hydroxyl group. It has been successfully employed in the inversion of various alcohols including carbohydrate derivatives.[20] The nucleophilic substitution of furanoside **6** with excess $NaNO_2$ at 120 °C for 5 h provided a 1:1 mixture of the expected inverted alcohol **7** and a side-product **7′** resulting from migration of the *p*-toluoyl group to the neighboring inverted C-3 hydroxyl group in moderate yield. Shortening the reaction time to 2 h gave a 4.5:1 regioisomeric mixture of **7**:**7′** in 58% yield. The sterically hindered C-3 hydroxyl group of **7** is much less reactive than the free C-5 hydroxyl group of **7′**, and therefore, benzoylation of the mixture facilitated the chromatographic purification of unreacted **7** from benzoylated **7′** in 89% recovery yield.

The C-3 hydroxyl group of **7** was next converted to the mesylate **8** in 90% yield. It is worth noting that attempts to perform Mitsunobu reaction of furanoside **4** with MeOTs or methanesulfonic acid to yield the mesylate with inverted configuration at C-3 gave only complex mixtures.[21] Reaction of **8** with excess NaN_3 at 90−100 °C for 2 h gave the expected azide **9** in 95% yield. Hydrogenation of **9** in the presence of Boc_2O gave the Boc-protected amine **10** in 71% yield as a white solid. Hydrolysis of *p*-toluoyl group in **10** followed by BAIB-TEMPO[22] oxidation gave the Boc-protected amino acid **12** in high yield. Treatment with trifluoroacetic acid (TFA) liberated

DOI: 10.1021/acs.joc.5b00890
J. Org. Chem. 2015, 80, 7058−7065

Table 1. Sequence and Characterization Data of atfcPNA

PNA	sequence (N→C)	N/C-terminal modification	t_R min[a]	m/z (calcd)[b]	m/z (found)[c]	yield %[d]
T9	TTTTTTTTT	Ac/LysNH$_2$	30.6	3198.2	3197.1	44
M10	GTAGATCACT	Ac/LysNH$_2$	25.1	3578.6	3578.4	22
M10Flu	GTAGATCACT	Flu/LysNH$_2$	28.4, 29.2	3894.8	3893.3	15
M10AT	TATGTACTAT	Bz/LysNH$_2$	29.1	3630.6	3630.7	20
M10CG	GCTACGTCGC	Bz/LysNH$_2$	28.1	3617.6	3617.9	10

[a]HPLC conditions: C18 column, 4.6 × 50 mm, 3 μ, gradient 0.1% TFA in H_2O:MeOH 90:10 for 5 min then linear gradient to 10:90 over 30 min, flow rate 0.5 mL/min, 260 nm. [b]Average mass of M + H$^+$. [c]MALDI-TOF. [d]Isolated yield after HPLC purification, spectrophotometrically determined.

Table 2. T_m of atfcPNA/acpcPNA and DNA/RNA

PNA (N→C)	DNA or RNA (5′→3′)	T_m atfcPNA (ΔT_m)[a]	T_m acpcPNA (ΔT_m)[a,b]	note
GTAGATCACT (**M10**)	dAGTGATCTAC	52.5	53.3	complementary DNA
	dAGTG<u>C</u>TCTAC	23.4 (−29.1)	23.8 (−29.5)	mismatched DNA
	dAGTG<u>G</u>TCTAC	23.4 (−29.1)	23.9 (−29.4)	mismatched DNA
	dAGTG<u>T</u>TCTAC	25.4 (−27.1)	29.4 (−23.9)	mismatched DNA
	dCATCTAGTGA	<20	<20	parallel DNA
	rAGUGAUCUAC	36.0	42.3	complementary RNA
	rAGUG<u>C</u>UCUAC	<20	23.6 (−18.7)	mismatched RNA
	rAGUG<u>G</u>UCUAC	<20	24.8 (−17.5)	mismatched RNA
	rAGUG<u>U</u>UCUAC	<20	<20	mismatched RNA
	rCAUCUAGUGA	<20	<20	parallel RNA
TATGTACTAT (**M10AT**)	dATAGTACATA	49.6	54.2	complementary DNA
	dATAG<u>A</u>ACATA	25.4 (−24.2)	23.4 (−30.8)	mismatched DNA
	dATAG<u>C</u>ACATA	30.2 (−19.4)	30.2 (−24.0)	mismatched DNA
	dATAG<u>G</u>ACATA	<20	24.4 (−29.8)	mismatched DNA
	dATACATGATA	<20	<20	parallel DNA
	rAUAGUACAUA	29.2	32.6	complementary RNA
	rAUACUAGAUA	<20	<20	parallel RNA
GCTACGTCGC (**M10CG**)	dGCGACGTAGC	56.4	54.5	complementary DNA
	dGCGA<u>A</u>GTAGC	23.4 (−33.0)	<20	mismatched DNA
	dGCGA<u>G</u>GTAGC	31.2 (−25.2)	30.2 (−24.3)	mismatched DNA
	dGCGA<u>T</u>GTAGC	36.0 (−20.4)	35.1 (−19.4)	mismatched DNA
	dCGATGCAGCG	<20	<20	parallel DNA
	rGCGACGUAGC	41.8	48.0	complementary RNA
	rCGAUGCAGCG	24.4 (−17.4)	39.2 (−8.8)	parallel RNA

[a]All T_m were measured at PNA = 1 μM, 100 mM NaCl, 10 mM sodium phosphate buffer, pH 7.0, heating rate 1 °C/min; and $\Delta T_m = T_m - T_m^{\text{complementary hybrid}}$ [b]The T_m data of acpcPNA are provided for comparison purposes. Except for the mismatched hybrids of **M10AT** and **M10CG**, T_m data of all acpcPNA hybrids were taken from ref 10d. Mismatch positions in DNA sequence are indicated by the underline.

the free amino acid which was further reacted with FmocOSu to give the desired Fmoc-protected amino acid **13** in 87% yield over 2 steps. Finally, the Fmoc-protected amino acid **13** was activated as its pentafluorophenyl (Pfp) ester **1** in 65% yield. The presence of the Pfp group was confirmed by ^{19}F NMR analysis. In summary, the target cyclic β-amino acid spacer (*SS*-ATFC) **1** was successfully synthesized from commercially available 2-deoxy-D-ribose (**2**) in a straightforward fashion over 11 steps in 6.7% overall yield.

Synthesis of atfcPNA. Four different sequences of atfcPNA (**T9**, **M10**, **M10AT**, and **M10CG**) were synthesized from the activated *SS*-ATFC spacer **1** and the four Fmoc-protected pyrrolidinyl PNA monomers (A^{Bz}, T, C^{Bz}, and G^{Ibu}) following the stepwise coupling protocol for Fmoc solid phase synthesis of PNA previously developed in our laboratory (Table 1).[10b] The atfcPNA sequences were end-capped at the *N*-termini by acetylation or benzoylation. In addition, an atfcPNA sequence (**M10**) was also end-capped with 5(6)-carboxyfluorescein to yield a **M10Flu** sequence in order to study nonspecific interactions. All atfcPNAs were purified by reverse phase HPLC and their identities were confirmed by MALDI-TOF mass spectrometry. In all cases, the PNAs were obtained with >90% purity, except for the **M10Flu** sequence which is split into two peaks on the HPLC chromatogram due to the presence of two carboxyfluorescein isomers. Isolated yields in the range of 10−44% were obtained, depending on the sequence. The poor isolated yields, which are typical for most solid phase syntheses, are attributed to the loss of product during HPLC purification due to separation issues rather than the synthetic efficiency. All PNAs are readily soluble in water (>1 mM). The sequences and characterization data of all atfcPNA are summarized in Table 1.

DNA and RNA Binding Properties of atfcPNA. Preliminary DNA binding studies were performed on the **T9** sequence. Since homopyrimidine/homopurine PNA sequences are known to form triplex structures, it is important to first determine the stoichiometry of binding. This was accomplished by UV titration (Figure S22 of the Supporting Information), which clearly confirms a 1:1 stoichiometry of atfcPNA:DNA as shown by the inflection point at ca. 50 mol % DNA. This is in agreement with other pyrrolidinyl PNA, whereby no $(PNA)_2$·

DOI: 10.1021/acs.joc.5b00890
J. Org. Chem. 2015, 80, 7058−7065

DNA triplex formation could be observed, presumably due to the bulkiness of the pyrrolidinyl PNA backbone.

Melting temperature measurements by UV spectrophotometry suggest that the **T9** atfcPNA binds cooperatively to its complementary DNA (dA_9), giving well-defined melting curves with melting temperatures (T_m) of 60.3 and 64.1 °C (in the presence and absence of 100 mM NaCl, respectively). These T_m figures are somewhat lower than the corresponding **T9** acpcPNA (T_m = 72.5 and >76.8 °C, in the presence and absence of 100 mM NaCl, respectively).[10d,e] Nevertheless, it is clear that **T9** atfcPNA can form a stable hybrid with its complementary DNA. In the presence of a mismatched base in the DNA strand, the T_m was dramatically decreased (−21.6, −21.9, and −31.8 °C for pT-dC, pT-dT, and pT-dG mismatches, respectively). The large decrease of T_m suggests that the atfcPNA binds to DNA with high specificity similar to that of acpcPNA.

Next, the DNA and RNA binding properties of mixed base atfcPNA were investigated and compared with the corresponding acpcPNA sequences (Table 2). Three sequences with different G+C content were compared (%G+C content: **M10AT** = 20; **M10** = 40; and **M10CG** = 70). As shown in Table 2, all atfcPNA sequences showed a strong DNA binding affinity, and specifically in antiparallel orientation similar to acpcPNA. They also exhibit very high sequence specificity as shown by a large decrease in T_m values of mismatched compared to the complementary hybrids ($\Delta T_m \sim 19–33$ °C), which are in the same range as acpcPNA ($\Delta T_m \sim 19–31$ °C) and are much more discriminating than aegPNA.[11] It is interesting to note that while acpcPNA·DNA hybrids did not show a definite relationship between T_m and the base composition,[10d] the T_m of atfcPNA showed a normal correlation with base composition (i.e., the T_m is increased with %G+C content). Further studies are clearly required in order to understand the basis of different behaviors between the two PNA systems, but it is beyond the scope of the present study.

In addition to DNA, atfcPNA can also bind to RNA in an antiparallel fashion, albeit with much lower affinity compared to the corresponding antiparallel DNA. Parallel hybrids with RNA were observed in G+C-rich sequences for both atfcPNA and acpcPNA, but the parallel hybrid was much less stable than the antiparallel hybrid, especially in the case of atfcPNA. Moreover, the RNA binding was highly sequence-specific as shown by a large decrease of T_m value in the presence of mismatched RNA targets. The normal correlation between T_m and base composition was again observed in atfcPNA·RNA hybrids. In addition, atfcPNA exhibits a greater selectivity for binding to DNA over RNA than acpcPNA as shown by the larger T_m difference between atfcPNA·RNA and atfcPNA·DNA hybrids (−20.4, −16.5, and −14.6 °C for **M10AT**, **M10**, and **M10CG**, respectively) compared to acpcPNA·RNA and acpcPNA·DNA hybrids (−21.6, −11.0, and −6.5 °C for **M10AT**, **M10**, and **M10CG**, respectively). Smaller differences were observed at higher G+C content in both PNA systems. The results suggest that atfcPNA and acpcPNA cannot effectively adjust themselves to the more limited conformational space of RNA duplexes exerted by the 2′-hydroxyl group in RNA, and that there are subtle differences between structures of A+T-rich and G+C-rich sequences.

Circular dichroism (CD) spectroscopy was also used to study the binding between the **T9** atfcPNA and DNA (Figure 1a). The **T9** atfcPNA exhibited weak CD signals in single-stranded form. The only prominent features were the positive band at 210 nm and a very small negative band at 280 nm. The single-stranded dA_9 DNA showed two minima at 206 and 250 nm and maxima at 220, 232 (shoulder), and 275 nm. Upon hybrid formation, the negative band at 250 nm was markedly intensified and shifted to a slightly shorter wavelength (248 nm). Moreover, significant changes were observed in the nucleobase absorption region (260–300 nm) as shown by the appearance of a new negative band at 268 nm and a positive band at 285 nm. These probably reflect a change in the orientation of the nucleobase, most likely as a result of base–base pairing and stacking in the atfcPNA·DNA duplex. The overall shape of the CD spectrum of atfcPNA·DNA hybrid is quite similar to the corresponding acpcPNA·DNA and DNA·DNA hybrid.[10b,d] It is therefore reasonable to assume that these hybrids adopt similar right-handed helical conformations. Heating caused the CD signal to return to the sum of the single-stranded components (Figure S23 of the Supporting Information). A plot of the CD signal at 248 nm as a function of temperature gave a sigmoidal curve (Figure S23 of the Supporting Information, inset). From this CD melting curve, a CD T_m of around 60 °C was obtained which is in good agreement to the T_m obtained by UV–vis spectrophotometry.

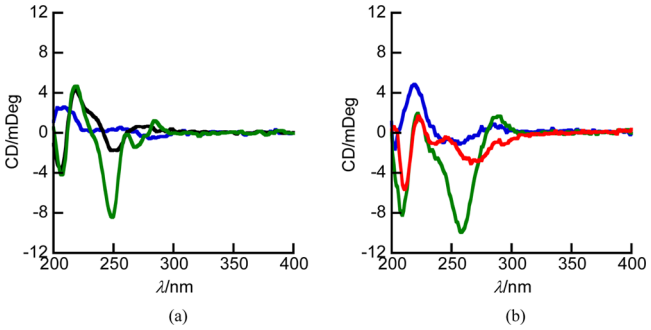

Figure 1. CD spectra of (a) **T9** atfcPNA (blue), dA_9 (black), and their 1:1 hybrid (green) and (b) **M10CG** atfcPNA (blue) and its hybrids with antiparallel DNA (green) or antiparallel RNA (red). Conditions: PNA = DNA = 2.5 μM in 10 mM sodium phosphate buffer (pH 7.0) and 100 mM NaCl at 20 °C.

In contrast to the homothymine sequence, CD spectra of single-stranded mixed base atfcPNA suggested pronounced intrastrand base stacking (Figure 1b, see also Figures S28–S30 of the Supporting Information). The CD spectra are remarkably similar to single-stranded DNA as shown by a negative band at 205 nm, a strong positive band at 220 nm, a negative band at 256–260 nm, and a positive band around 280 nm with a crossover point around 267–273 nm.[23] Hybridization with antiparallel DNA did not change the overall shape of the CD spectra. However, the negative band at 260 nm became more intense and slightly shifted toward a longer wavelength. These are in agreement with tightening of the helical pitch after duplex formation.[14] The effect is most clearly observed in the G+C-rich sequence **M10CG**. The overall shape of the CD spectra of atfcPNA·DNA hybrids corresponds to the B-form of DNA·DNA duplexes.[24] On the other hand, CD spectra of atfcPNA·RNA hybrids exhibited distinct features in the 250–300 nm region (Figure 1b, see also Figures S28–S30 of the Supporting Information). A positive band was observed between 245–256 nm together with a negative band with minima around 265 nm. This suggests that the atfcPNA·DNA and atfcPNA·RNA hybrids adopt different conformations, which could contribute to their different stabilities.

DOI: 10.1021/acs.joc.5b00890
J. Org. Chem. 2015, 80, 7058–7065

The shorter C−O bond as well as the presence of lone pair electrons in atfcPNA resulted in reduced steric effects compared to acpcPNA. It may also provide an additional potential hydrogen-bonding site and repulsion with the negatively charged phosphate group in the DNA/RNA strand. These factors could potentially contribute to the subtle difference in nucleic acid binding properties of atfcPNA and acpcPNA. An NMR study of oligomers of the opposite enantiomer (2*R*,3*R*) of *trans*-atfc suggested torsional angle (θ) values in the range of 52−64° based on coupling constant ($^3J_{H-H}$) analyses.[13a] These values are much smaller than the optimal values obtained from MD simulations of acpcPNA·DNA hybrids (99−102°).[11] The fact that atfcPNA can still form stable hybrids with DNA suggests that the tetrahydrofuran ring should be sufficiently flexible to adopt the required torsional angle. On the basis of NMR experiments, no evidence of intramolecular hydrogen bonding between the amide bonds and the oxygen atom of the atfc ring was observed in *trans*-atfc oligomers.[13a] However, this does not rule out the possibilities of interstrand hydrogen bonding and/or additional interactions such as repulsion with the phosphate group of DNA or RNA. The absence of detailed three-dimensional structures of atfcPNA and its DNA/RNA hybrids precludes us from drawing a more definite conclusion.

Solubility and Nonspecific Binding Properties of atfcPNA versus acpcPNA. It was expected that the replacement of the cyclopentane ring in acpcPNA with the hydrophilic tetrahydrofuran ring in atfcPNA should result in a less hydrophobic PNA backbone. The more polar nature of atfcPNA is evidenced in the decreased retention time from reverse-phase HPLC analyses (**T9**: atfcPNA 30.6 min, acpcPNA 33.3 min; **M10**: atfcPNA 25.1 min, acpcPNA 30.0 min) (Figures S14, S19, S15, and S20 of the Supporting Information). Due to the small synthesis scale, it was not possible to directly compare the solubility because all lysine-modified PNA sequences are readily soluble in water and saturation could not be achieved. Acetylation of the C-terminal lysine modifier allowed the comparison of solubility between **T9** acpcPNA and atfcPNA. Unfortunately, the solubility of **T9** atfcPNA was only marginally improved (425 ± 21 μM or ca. 1.4 mg/mL) over **T9** acpcPNA (348 ± 10 μM or ca. 1.1 mg/mL). This unexpected solubility behavior might be interpreted in terms of a combination between stable packing of the PNA molecules in the solid state and unfavorable entropy of dissolution as proposed to explaining the low aqueous solubility of cellulose[25] and cyclodextrins.[26]

Similar to conventional PNA,[14] nonspecific binding with hydrophobic materials was occasionally observed with acpcPNA. This becomes a serious problem when the PNA is modified with one or more hydrophobic dyes. To compare the nonspecific binding behaviors of atfcPNA and acpcPNA, *N*-terminal fluorescein-labeled atfcPNA and acpcPNA **M10Flu** were synthesized and compared. Both fluorescein-labeled PNAs form stable hybrids with their complementary DNA target with T_m of 45.7 and 46.7 °C, respectively. The nonspecific adsorption of the fluorescein-labeled PNAs by two different brands of polypropylene plastic tubes were investigated (Figure 2a). Fluorescence measurements of PNA solutions (50 nM) were recorded before and after repeated transfer between the plastic tube and the cuvette until there was no further change in the fluorescence intensity. It was observed that the acpcPNA signal decreased quite significantly (80.1 ± 3.6 and 53.3 ± 2.3% of the original value for brands 1 and 2, respectively), while the atfcPNA signal does not change as much (95.8 ± 3.6 and 105.8 ± 1.4% of the original value for brands 1 and 2, respectively).

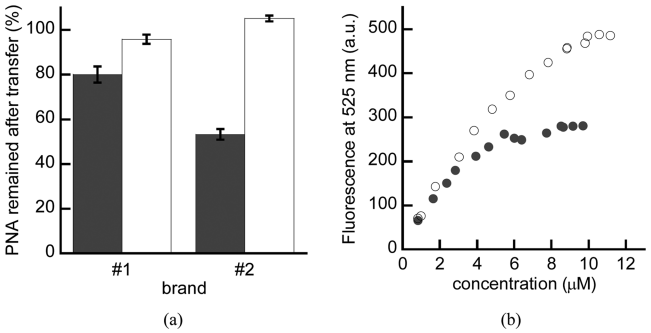

Figure 2. Comparison of fluorescein-labeled acpcPNA (gray) and atfcPNA (white) (**M10Flu**) for (a) nonspecific adsorption onto polypropylene microcentrifuge tube and (b) self-aggregation as demonstrated by fluorescence spectrophotometry.

Reduction of the nonspecific self-aggregation of **M10Flu** atfcPNA was further demonstrated by fluorescence spectroscopy (Figure 2b). At low concentrations (≤1 μM), both PNAs showed comparable fluorescence. However, at higher concentrations, the fluorescence of **M10Flu** acpcPNA was significantly lower and reached a plateau at concentrations above 5 μM due to self-aggregation of the PNA, resulting in self-quenching of the fluorescein label. The same leveling effect was also observed in **M10Flu** atfcPNA but at twice as high a concentration. Accordingly, at 10 μM, the fluorescence of **M10Flu** atfcPNA is 70% brighter than acpcPNA at the same concentration. Addition of complementary DNA to **M10Flu** acpcPNA and to atfcPNA restored the fluorescence of both PNAs to the same level due to repulsion between the negatively charged PNA·DNA hybrids, which separated the fluorescein dyes from each other. These results support the beneficial effects of the hydrophilic ATFC spacer in reducing nonspecific interactions of pyrrolidinyl PNA, which should further expand the applications of these PNAs.

■ CONCLUSION

In conclusion, we report an efficient synthesis of Fmoc-protected tetrahydrofuran cyclic-β-amino acid from 2-deoxy-D-ribose. The cyclic amino acid was successfully incorporated as a building block for synthesizing a new tetrahydrofuran-containing pyrrolidinyl PNA (atfcPNA). This novel atfcPNA retained the excellent DNA binding affinity and specificity of pyrrolidinyl PNA, with improved selectivity toward hybridization to DNA over RNA, a fact that is interesting in its own right and should deserve further investigation in the context of development of a selective DNA binding agent. In addition, the hydrophilic tetrahydrofuran backbone provided beneficial effects in reducing nonspecific interactions and self-aggregation generally observed in acpcPNA and most other PNA systems.

■ EXPERIMENTAL SECTION

General Methods. All chemicals were purchased from commercial sources and were used as received without further purification. Solvents were dried over CaH_2 or 4 Å molecular sieves and then freshly distilled under argon prior to use. IR spectra were acquired on a FT-IR spectrometer using either attenuated total reflection (ATR) or transmission module. Optical rotations ($[\alpha]_D$) were measured at the specified temperature using sodium light (D line, 589.3 nm); concentrations (c) are reported as g/100 mL. ^{1}H and ^{13}C NMR spectra were recorded at 400 and 100 MHz, respectively. High-

DOI: 10.1021/acs.joc.5b00890
J. Org. Chem. 2015, 80, 7058−7065

resolution mass spectra (HRMS) were recorded in electrospray ionization-time-of-flight (ESI-TOF) mode. MALDI-TOF mass spectra of all atfcPNAs were obtained in linear positive ion mode using α-cyano-4-hydroxy cinnamic acid (CCA) as a matrix.

*Methyl 2-Deoxy-D-ribofuranoside (**3**) (Mixture of α and β Anomers).* Methyl 2-deoxy-D-ribofuranoside **3** was synthesized according to the literature procedure with a slight modification on the catalyst quantity and reaction time.[16,17] 2-Deoxy-D-ribose (11.4 g, 85.0 mmol) was dissolved in anhydrous methanol (55 mL) under a nitrogen atmosphere, and then methanesulfonic acid (0.27 mL, 4.16 mmol) was added at room temperature. The reaction reached completion after stirring for 30 min at room temperature as confirmed by TLC analysis (CH_2Cl_2:MeOH 9:1, *p*-anisaldehyde stain; R_f = 0.42). The reaction was then quenched by portionwise addition of 4-(*N*,*N*-dimethylamino)pyridine (DMAP) (1.02 g, 8.35 mmol). The reaction mixture was concentrated under reduced pressure by azeotropic distillation with toluene to afford a brown syrup (14.15 g, >90% purity by TLC), which was used for the next steps without further purification.

*Methyl 5-O-p-toluoyl-2-deoxy-D-ribofuranoside (**4**) (Mixture of α and β Anomers).* *p*-Toluoyl chloride (13 mL, 98.3 mmol) dissolved in anhydrous CH_2Cl_2 (20 mL) was added dropwise to a solution of crude **3** (prepared from 85.0 mmol of **2**) in 1:3 anhydrous pyridine/CH_2Cl_2 (80 mL) at 0 °C and stirred for 5 h. The reaction mixture was then diluted with CH_2Cl_2 (20 mL) and washed with cold H_2O (2 × 50 mL) and 5% aqueous $CuSO_4$. The combined organic extracts were washed with saturated $NaHCO_3$ (2 × 50 mL), followed by 2 M HCl (2 × 50 mL), and then dried over Na_2SO_4 and concentrated under reduced pressure to afford a brown syrup (21.64 g). The crude product was purified by column chromatography on silica gel to yield compound **4** as a colorless oil (15.1 g, 56.8 mmol, 67% yield from **2**). TLC analysis (hexanes:EtOAc 3:2; *p*-anisaldehyde stain; R_f = 0.27). $[\alpha]_D^{24}$ +67° (*c* 0.5, $CHCl_3$). IR (thin film): 3467.5, 2949.5, 2917.7, 2828.0, 1716.7, 1609.7, 1447.6, 1268.2, 1181.4, 1077.2, 842.8, 758.8 cm^{-1}. ^1H NMR (400 MHz, $CDCl_3$) (major isomer): δ 7.92 (d, *J* = 8.2 Hz, 2H), 7.25 (d, *J* = 8.1 Hz, 4H), 5.16 (m, 1H), 4.32−4.41 (m, 3H), 4.26 (m, 1H), 3.42 (s, 3H), 3.01 (m, 1H), 2.43 (s, 3H), 2.20 (m, 1H), 2.08 (m, 1H). ^{13}C NMR (100 MHz, $CDCl_3$) (major isomer): δ 166.4, 143.9, 129.7, 129.1, 127.0, 105.5, 85.1, 73.1, 64.4, 54.9, 40.9, 21.6. HRMS (ESI+): *m*/*z* calcd for $C_{14}H_{18}O_5Na$ [M + Na^+], 289.1052; found, 289.1061.

*Methyl 5-O-p-toluoyl-3-O-tosyl-2-deoxy-D-ribofuranoside (**5**).* A solution of **4** (4.26 g, 16.0 mmol) and DMAP (183 mg, 1.5 mmol) in anhydrous CH_2Cl_2 (10 mL) was cooled to 0 °C under a N_2 atmosphere and then treated with Et_3N (5.00 mL, 35.8 mmol) and a solution of TsCl (4.011 g, 21.0 mmol) in CH_2Cl_2 (5 mL). The reaction mixture was allowed to warm to room temperature and monitored by TLC (hexanes:EtOAc 3:2; *p*-anisaldehyde stain; R_f = 0.42). After completion, the reaction mixture was quenched at 0 °C with 2 M HCl, neutralized with saturated aqueous $NaHCO_3$ and extracted with EtOAc. The combined organic extracts were washed with water (40 mL), brine (40 mL), dried over Na_2SO_4, and evaporated. The crude product (6.40 g) was purified by column chromatography on silica gel to afford compound **5** (5.59 g, 13.3 mmol, 83%). $[\alpha]_D^{24}$ +75° (*c* 0.5, $CHCl_3$). IR (thin film): 3027.6, 2949.5, 2929.3, 2836.7, 1922.2, 1716.7, 1606.8, 1450.5, 1363.7, 1276.8, 1172.7, 1106.1, 1056.9, 984.6, 920.9, 848.5, 810.9, 753.0, 666.2, 567.8, 550.5 cm^{-1}. ^1H NMR (400 MHz, $CDCl_3$): δ 7.85 (d, *J* = 8.0 Hz, 2H), 7.77 (d, *J* = 8.3 Hz, 2H), 7.27 (d, *J* = 8.3 Hz, 2H), 7.24 (d, *J* = 8.0 Hz, 2H), 5.06 (m, 1H), 4.93 (m, 1H), 4.38−4.44 (m, 2H), 4.20 (m, 1H), 3.36 (s, 3H), 2.42 (s, 3H), 2.39 (s, 3H), 2.34 (m, 1H), 2.13 (m, 1H). ^{13}C NMR (100 MHz, $CDCl_3$): δ 166.0, 145.1, 144.0, 133.4, 129.9, 129.7, 129.1, 127.9, 126.9, 104.5, 80.1, 79.4, 63.0, 55.1, 39.2, 21.7, 21.6. HRMS (ESI+): *m*/*z* calcd for $C_{21}H_{24}O_7SNa$ [M + Na^+], 443.1135; found, 443.1137.

*5-O-p-toluoyl-3-O-tosyl-1,2-dideoxy-D-ribose (**6**).* A solution of compound **5** (2.41 g, 5.73 mmol) in anhydrous CH_2Cl_2 (2 mL) was cooled to 0 °C and treated with Et_3SiH (2.90 mL, 18.2 mmol), followed by dropwise addition of $BF_3{\cdot}OEt_2$ (2.00 mL, 16.2 mmol). The progress of the reaction was monitored by TLC (Hexanes:EtOAc 1:1; negative *p*-anisaldehyde stain; R_f = 0.58). After completion, the reaction mixture was neutralized with saturated aqueous $NaHCO_3$ (30 mL) and extracted with CH_2Cl_2 (3 × 10 mL). The combined organic extracts were dried over Na_2SO_4 and evaporated. The crude product (2.31 g) was purified by column chromatography to afford compound **6** as a colorless oil (1.92 g, 4.92 mmol, 86%). $[\alpha]_D^{23}$ +30° (*c* 1.0, CH_2Cl_2). IR (thin film): 2958.2, 2880.1, 1716.8, 1606.8, 1447.6, 1363.7, 1268.2, 1172.7, 1091.6, 1016.4, 955.6, 906.4, 816.7, 753.0, 669.1, 553.4 cm^{-1}. ^1H NMR (400 MHz, $CDCl_3$): δ 7.87 (d, *J* = 8.3 Hz, 2H), 7.77 (d, *J* = 8.1 Hz, 2H), 7.28 (d, *J* = 8.2 Hz, 2H), 7.24 (d, *J* = 8.1 Hz, 2H), 5.00 (m, 1H), 4.15−4.25 (m, 3H), 4.05 (m, 1H), 3.94 (m, 1H), 2.42 (s, 3H), 2.40 (s, 3H), 2.15−2.20 (m, 2H). ^{13}C NMR (100 MHz, $CDCl_3$): δ 166.1, 145.1, 144.0, 133.6, 130.0, 129.7, 129.2, 127.8, 126.9, 82.2, 81.6, 67.4, 63.6, 33.1, 21.7, 21.6. HRMS (ESI+): *m*/*z* calcd for $C_{20}H_{22}O_6SNa$ [M + Na^+], 413.1029; found, 413.1026.

*[(2R,3R)-3-Hydroxytetrahydrofuran-2-yl]methyl-4-methylbenzoate (**7**).* A mixture of compound **6** (1.08 g, 2.77 mmol) and $NaNO_2$ (0.96 g, 13.9 mmol) in DMSO (10 mL) was heated to 120 °C for 5 h. After completion as monitored by TLC analysis (hexanes:EtOAc 1:1; R_f = 0.27), the reaction was diluted with water. The aqueous layer was then extracted with CH_2Cl_2 (3 × 10 mL) and the combined organic extracts were washed with brine, dried over Na_2SO_4, and evaporated. The crude product was purified by column chromatography to afford a mixture of **7** and the toluoyl migrate product **7′** in a 1:1 ratio as determined by NMR analysis (0.41 g, 1.75 mmol, combined yield 63%). When the reaction time was reduced to 2 h at 120 °C, the product was obtained as 4.5:1 regioisomeric mixture of product **7**:**7′** in 58% combined yield.

For characterization purposes, the 1:1 regioisomeric mixture from the experiment above (0.41 g, 1.75 mmol) was dissolved in anhydrous CH_2Cl_2 (3 mL), cooled to 0 °C, and then treated with Et_3N (1.25 mL, 8.96 mmol) and Bz_2O (0.3370 g, 1.49 mmol). The reaction mixture was concentrated to dryness and purified by column chromatography to yield **7** as colorless oil (0.18 g, 0.76 mmol, 28% overall yield from **6**). This corresponds to a 89% recovery from the mixture. Mp: 65−67 °C; $[\alpha]_D^{23}$ −4° (*c* 1, CH_2Cl_2). IR (ATR) 3420.7, 2986.2, 2950.6, 2923.3, 2896.0, 2868.7, 1704.4, 1611.5, 1444.7, 1269.8, 1174.2, 1100.4, 1021.1, 969.2, 834.5, 750.6, 693.2 cm^{-1}. ^1H NMR (400 MHz, $CDCl_3$): δ 7.94 (d, *J* = 8.2 Hz, 2H), 7.24 (d, *J* = 8.0 Hz, 2H), 4.77 (dd, *J* = 7.1, 11.6 Hz, 1H), 4.34−4.39 (m, 2H), 4.11 (m, 1H), 3.96 (ddd, *J* = 3.3, 5.4, 7.1 Hz, 1H), 3.89 (dt, *J* = 3.8, 8.6 Hz, 1H), 2.41 (s, 3H), 2.18 (m, 1H), 2.05 (m, 1H). ^{13}C NMR (100 MHz, $CDCl_3$): δ 167.2, 144.1, 129.8, 129.2, 126.9, 80.6, 71.5, 66.5, 62.6, 35.1, 21.7. HRMS (ESI+): *m*/*z* calcd for $C_{13}H_{16}O_4Na$ [M + Na^+], 259.0946; found, 259.0941.

*[(2R,3R)-3-(Methylsulfonyloxy)tetrahydrofuran-2-yl]methyl 4-methylbenzoate (**8**).* A solution of **7** (0.49 g, 2.07 mmol) in anhydrous CH_2Cl_2 (4 mL) was cooled to 0 °C and treated with DMAP (50 mg, 0.41 mmol), Et_3N (1.15 mL, 8.25 mmol), and MsCl (0.48 mL, 6.20 mmol). After 1 h, the reaction was complete as indicated by TLC (CH_2Cl_2:acetone 4:1; R_f = 0.76) and was diluted with H_2O (10 mL) and EtOAc (10 mL). The aqueous layer was extracted with EtOAc (3 × 10 mL), and the combined organic extracts were washed with brine, dried over Na_2SO_4, and concentrated under reduced pressure. The crude product (0.62 g) was purified by column chromatography to afford **8** as a white solid (0.58 g, 1.85 mmol, 90%). Mp: 102−104 °C. $[\alpha]_D^{23}$ −44° (*c* 1.0, CH_2Cl_2). IR (KBr): 3424.1, 3024.8, 2964.0, 2940.8, 2891.6, 2862.7, 1722.5, 1609.6, 1349.2, 1271.1, 1178.5, 1109.0, 1010.6, 967.2, 897.7, 750.2, 524.4 cm^{-1}. ^1H NMR (400 MHz, $CDCl_3$): 7.94 (d, *J* = 7.8 Hz, 2H), 7.24 (d, *J* = 8.1 Hz, 2H), 5.38 (m, 1H), 4.53 (m, 2H), 4.25 (dt, *J* = 4.0, 6.1 Hz, 1H), 4.15 (m, 1H), 3.96 (dt, *J* = 2.7, 8.5 Hz, 1H), 3.01 (s, 3H), 2.41 (s, 3H), 2.39 (m, 2H). ^{13}C NMR (100 MHz, $CDCl_3$): δ 166.2, 144.0, 129.8, 129.2, 127.0, 79.9, 78.8, 66.5, 62.2, 38.5, 34.0, 21.7; HRMS (ESI+): *m*/*z* calcd for $C_{14}H_{18}O_6SNa$ [M + Na^+], 337.0722; found, 337.0716.

*[(2S,3S)-3-Azidotetrahydrofuran-2-yl]methyl-4-methylbenzoate (**9**).* A solution of **8** (0.14 g, 0.46 mmol) in DMSO (2 mL) was treated with NaN_3 (0.21 g, 3.15 mmol) and then heated at 90 °C for 2 h. After the reaction reached completion as monitored by TLC analysis (hexanes:EtOAc 3:2; R_f = 0.62), it was diluted with water (15 mL) and extracted with EtOAc (3 × 15 mL). The combined organic extracts were dried over Na_2SO_4 and concentrated to dryness to afford compound **9** as a colorless oil (113 mg, 0.43 mmol, 95%), which was subjected to the next step without further purification. $[\alpha]_D^{23}$ +64° (*c*

DOI: 10.1021/acs.joc.5b00890
J. Org. Chem. 2015, 80, 7058−7065

1.6, CH_2Cl_2). IR (thin film): 2952.4, 2872.4, 2098.7, 1716.7, 1606.7, 1271.1, 1172.7, 1103.2, 750.2 cm^{-1}. ^1H NMR (400 MHz, $CDCl_3$): δ 7.93 (d, J = 8.0 Hz, 2H), 7.25 (d, J = 8.0 Hz, 2H), 4.38 (m, 2H), 4.03−4.12 (m, 3H), 3.95 (m, 1H), 2.42 (s, 3H), 2.29 (m, 1H), 2.08 (m, 1H). ^{13}C NMR (100 MHz, $CDCl_3$): δ 166.3, 144.0, 129.7, 129.2, 127.0, 81.5, 67.4, 64.4, 62.9, 32.2, 21.7. HRMS (ESI+): m/z calcd for $C_{13}H_{15}N_3O_3Na$ [M + Na^+], 284.1006; found, 284.1003.

*[(2S,3S)-3-(tert-Butoxycarbonylamino)tetrahydrofuran-2-yl]-methyl 4-methylbenzoate (**10**).* A solution of **9** (0.47 g, 1.8 mmol) in MeOH (5 mL) was treated with Boc_2O (1.03 g, 4.72 mmol) and Pd/C (20% w/w, 74.2 mg). The reaction flask was flushed with H_2 gas and a H_2 balloon was attached through a rubber septum. The reaction was monitored by TLC analysis (hexanes:EtOAc 3:2; ninhydrin stain; R_f = 0.46) until it reached completion. It was then filtered through Celite, concentrated to dryness, and the residue was washed with hexanes to afford **10** as a white solid (0.43 g, 1.28 mmol, 71%). Mp: 108−110 °C. $[\alpha]_D^{23}$ +28° (c 1.0, CH_2Cl_2). IR (KBr): 3348.9, 2975.6, 2937.9, 2868.5, 1724.8, 1682.0, 1609.0, 1528.6, 1432.5, 1369.5, 1271.1, 1172.7, 1108.3, 1077.2, 1021.5, 1001.2, 882.6, 884.9, 753.1, 607.6 cm^{-1}. ^1H NMR (400 MHz, $CDCl_3$): δ 7.93 (d, J = 8.2 Hz, 2H), 7.22 (d, J = 8.1 Hz, 2H), 4.71 (br s, 1H), 4.49 (dd, J = 3.5, 11.7 Hz, 1H), 4.34 (dd, J = 5.9, 11.8 Hz, 1H), 4.16 (m, 1H), 3.92−4.06 (m, 3H), 2.40 (s, 3H), 2.34 (m, 1H), 1.83 (dt, J = 5.7, 12.8 Hz, 1H), 1.44 (s, 9H). ^{13}C NMR (100 MHz, $CDCl_3$): δ 166.5, 155.5, 143.7, 129.8, 129.1, 127.2, 82.9, 79.9, 67.2, 65.1, 53.2, 33.3, 28.4, 21.6. HRMS (ESI+): m/z calcd for $C_{18}H_{25}NO_5Na$ [M + Na^+], 358.1625; found, 358.1635.

*tert-Butyl (2S,3S)-2-(Hydroxymethyl)tetrahydrofuran-3-ylcarbamate (**11**).* A mixture of **10** (0.39 g, 1.16 mmol) and LiOH·H_2O (0.13 g, 3.1 mmol) was dissolved in 1:1 THF:H_2O (4 mL) and stirred at room temperature overnight. The completion of the reaction was confirmed by TLC analysis (EtOAc:hexanes 4:1; ninhydrin stain; R_f = 0.33), and then the organic solvent was removed by rotary evaporation, and the aqueous residue was extracted with CH_2Cl_2 (3 × 10 mL). The combined organic phases were dried over anhydrous Na_2SO_4 and evaporated to give compound **11** as a white solid (0.23 g, 1.06 mmol, 91%). Mp: 85−87 °C. $[\alpha]_D^{23}$ −11° (c 1.0, CH_2Cl_2). ^1H NMR (400 MHz, $CDCl_3$): δ 4.47 (s, 1H), 3.85−4.00 (m, 3H), 3.65−3.69 (m, 3H), 2.87 (s, 1H), 2.29 (m, 1H), 1.79 (m, 1H), 1.44 (s, 9H). ^{13}C NMR (100 MHz, $CDCl_3$): δ 155.9, 85.1, 80.2, 66.7, 63.1, 52.9, 33.1, 28.3. IR (ATR): 3346.8, 2987.4, 2964.1, 2908.1, 2849.5, 1676.0, 1522.0, 1363.3, 1300.3, 1239.6, 1160.3, 1097.3, 1073.9, 1015.6, 866.3, 621.2 cm^{-1}. HRMS (ESI+): m/z calcd for $C_{10}H_{19}NO_4Na$ [M + Na^+], 240.1206; found, 240.1207.

*(2S,3S)-3-(tert-Butoxycarbonylamino)tetrahydrofuran-2-carboxylic acid (**12**).* To a solution of **11** (0.27 g, 1.24 mmol) in 1:1 acetonitrile:H_2O was added TEMPO (95 mg, 0.61 mmol) and bis(acetoxy)iodobenzene (BAIB) (1.13 g, 3.5 mmol). The reaction mixture was stirred overnight at room temperature. The completion of the reaction was monitored by TLC analysis (EtOAc; ninhydrin stain; R_f = 0.17). The pH of the resulting solution was adjusted 8−9 by addition of solid $NaHCO_3$ and extracted with EtOAc. The collected aqueous phase was acidified to pH 2 with solid $NaHSO_4$ followed by extraction with EtOAc. The combined organic phases were evaporated to dryness to give **12** as a colorless oil (0.27 g, 1.2 mmol, 94%). $[\alpha]_D^{22}$ +49° (c 1.5, DMSO). IR (thin film): 3328.6, 2972.7, 1710.9, 1528.6, 1363.7, 1279.7, 1161.1, 1100.3, 1016.4 cm^{-1}. ^1H NMR (400 MHz, DMSO-d_6): δ 12.60 (br s, 1H), 7.27 (d, J = 6.9 Hz, 1H), 4.10 (m, 1H), 4.04 (m, 1H), 3.83−3.92 (m, 2H), 2.06 (m, 1H), 1.76 (dt, J = 6.3, 12.0 Hz, 1H), 1.38 (s, 9H). ^{13}C NMR (100 MHz, DMSO-d_6): δ 172.7, 154.9, 81.0, 77.9, 67.1, 54.9, 31.6, 28.1. HRMS (ESI+): m/z calcd for $C_{10}H_{17}NO_5Na$ [M + Na^+], 254.0999; found, 254.0992.

*(2S,3S)-3-{[(9H-Fluoren-9-yl)methoxy]carbonylamino}tetrahydrofuran-2-carboxylic acid (**13**).* Compound **12** (0.21 g, 0.91 mmol) was dissolved in 1:1 TFA:CH_2Cl_2 (6 mL) and stirred at room temperature for 30 min. The solvent was removed by flushing with N_2. The crude amino acid was dissolved in H_2O (4 mL), and the pH of the solution was adjusted to 8−9 by the addition of solid $NaHCO_3$. Next, FmocOSu (0.31 g, 0.92 mmol) dissolved in 0.5 mL of DMSO was added in small portions along with more $NaHCO_3$ to maintain the pH around 8−9. To this mixture, MeCN was added to make a homogeneous solution. After stirring overnight, the solution was diluted with water and extracted with diethyl ether. The aqueous phase was acidified to pH 2 with concentrated HCl to give a white suspension. After filtration, the precipitate was air-dried to afford compound **13** as a white solid (0.28 g, 0.79 mmol, 87%). Mp: 166−168 °C. $[\alpha]_D^{23}$ +42° (c 1.0, DMSO). IR (KBr): 3308.4, 3062.4, 2946.6, 2362.1, 2341.8, 1722.5, 1690.7, 1540.2, 1447.6, 1259.6, 1099.4, 732.8 cm^{-1}. ^1H NMR (400 MHz, DMSO-d_6): δ 12.75 (br s, 1H), 7.89 (d, J = 7.4 Hz, 2H), 7.74 (d, J = 7.5 Hz, 1H), 7.69 (m, 2H), 7.42 (t, J = 7.0 Hz, 2H), 7.34 (t, J = 7.0 Hz, 2H), 4.33 (d, J = 6.4 Hz, 2H), 4.22 (t, J = 6.9 Hz, 1H), 4.17 (m, 1H), 4.09 (m, 1H), 3.90 (t, J = 6.8 Hz, 2H), 2.09 (m, 1H), 1.79 (m, 1H). ^{13}C NMR (100 MHz, DMSO-d_6): δ 172.8, 155.5, 143.7, 140.6, 127.5, 127.0, 125.0, 120.0, 81.1, 67.0, 65.3, 55.3, 46.6, 31.8. HRMS (ESI+): m/z calcd for $C_{20}H_{19}NO_5Na$ [M + Na^+], 376.1155; found, 376.1180.

*Pentafluorophenyl (2S,3S)-3-{[(9H-fluoren-9-yl)methoxy]-carbonylamino}tetrahydrofuran-2-carboxylate (**1**).* A suspension of compound **13** (0.22 g, 0.62 mmol) in CH_2Cl_2 (2 mL) was treated with DIEA (600 μL, 3.45 mmol) and PfpOTfa (600 μL, 3.39 mmol) in three portions. The completion of the reaction was monitored by TLC analysis (hexanes:EtOAc 1:1; R_f = 0.50). The reaction mixture was diluted with CH_2Cl_2 (10 mL), washed with 1 M HCl and saturated aqueous $NaHCO_3$ and dried over anhydrous Na_2SO_4. After removal of the solvent, the resulting pink oil was sonicated with hexanes to give a white suspension which was collected by filtration to give **1** as a white solid (0.207 g, 0.40 mmol, 65%). Mp: 123−125 °C. $[\alpha]_D^{23}$ +57° (c 1.0, CH_2Cl_2). IR (ATR): 3309.4, 1799.7, 1687.6, 1550.0, 1519.6, 1291.0, 1234.9, 1066.9, 1031.9, 994.6, 761.2, 735.6, 665.6. ^1H NMR (400 MHz, $CDCl_3$): δ 7.77 (d, J = 7.4 Hz, 2H), 7.58 (d, J = 7.2 Hz, 2H), 7.41 (t, J = 6.9 Hz, 2H), 7.31 (t, J = 7.1 Hz, 2H), 5.06 (d, J = 5.3, 1H), 4.70 (m, 1H), 4.62 (m, 1H), 4.50 (m, 2H), 4.19 (m, 2H), 4.12 (m, 1H), 2.36 (m, 1H), 1.98 (m, 1H). ^{13}C NMR (100 MHz, $CDCl_3$): δ 167.3, 155.5, 143.7, 141.4, 127.8, 127.0, 124.9, 120.0, 81.7, 68.3, 66.9, 56.2, 47.3, 31.9. ^{19}F NMR (376 MHz, $CDCl_3$): δ −161.8 (t, J = 20.2 Hz), −157.1 (t, J = 19.9 Hz), −152.4 (d, J = 18.0 Hz). HRMS (ESI+) m/z calcd for $C_{26}H_{18}F_5NO_4K$ [M + K^+], 542.0788; found, 542.0795.

Synthesis of atfcPNA. All atfcPNA were manually synthesized at 1.5 μmol scale on a Tentagel S-RAM resin (0.24 mmol/g loading) from the four Fmoc-protected pyrrolidinyl PNA monomers (A^{Bz}, T, C^{Bz}, and G^{Ibu}) and pentafluorophenyl-activated ATFC spacer 1 following the previously published protocol for acpcPNA synthesis.[10b,d] The nucleobase protecting groups (Bz, Ibu) were removed by treating the resin with 1:1 aqueous ammonia:dioxane at 60 °C overnight. The crude PNA was obtained by TFA cleavage and purified by reverse-phase HPLC (C18 column, 0.1% TFA in water−methanol gradient).

Fluorescence Spectroscopy to Compare Nonspecific Interactions and Self-Aggregation of acpcPNA and atfcPNA. (a) Nonspecific adsorption of fluorescein-modified acpcPNA and atfcPNA **M10Flu** were compared by fluorescence measurements. The PNA samples were prepared at 0.05 μM in 10 mM sodium phosphate buffer pH 7.0 (1000 μL) at 25 °C. The solution was transferred back and forth between the cuvette and a 1.5 mL polypropylene microcentrifuge tube, and the fluorescence spectra were recorded after each transfer until no further change was observed. The average fluorescence at 520 nm and standard deviation were calculated from the last three measurements after the signal was constant. The excitation wavelength was 480 nm, slit widths 5 nm, and the PMT voltage was set to high. (b) Self-aggregation of fluorescein-modified acpcPNA and atfcPNA **M10Flu** were compared by fluorescence measurements. The fluorescence data was plotted against concentration in the range of 1 to 10 μM or until a plateau was reached. The excitation wavelength was 480 nm, slit widths 5 nm, and the PMT voltage was set to 500.

■ ASSOCIATED CONTENT

Ⓢ Supporting Information

^1H and ^{13}C NMR spectra for numbered compounds, HPLC chromatogram, and MALDI-TOF mass spectra of PNA, as well as additional spectroscopic data. The Supporting Information is

DOI: 10.1021/acs.joc.5b00890
J. Org. Chem. 2015, 80, 7058−7065

available free of charge on the ACS Publications website at DOI: 10.1021/acs.joc.5b00890.

AUTHOR INFORMATION

Corresponding Author

*E-mail: vtirayut@chula.ac.th.

Notes

The authors declare no competing financial interest.

ACKNOWLEDGMENTS

Financial support of this work provided by the Thailand Research Fund (DPG5780002) and the Thai government stimulus package 2 (TKK2555, SP2) under the Project for Establishment of Comprehensive Center for Innovative Food, Health Products and Agriculture is gratefully acknowledged. We thank Haruthai Pansuwan and Nattawut Yotapan for partial data collection.

REFERENCES

(1) (a) Gellman, S. H. *Acc. Chem. Res.* **1998**, *31*, 173−180. (b) Hill, D. J.; Mio, M. J.; Prince, R. B.; Hughes, T. S.; Moore, J. S. *Chem. Rev.* **2001**, *101*, 3893−4011.

(2) (a) Fülöp, F. *Chem. Rev.* **2001**, *101*, 2181−2204. (b) Fülöp, F.; Martinek, T. A.; Tóth, G. K. *Chem. Soc. Rev.* **2006**, *35*, 323−334.

(3) (a) Cheng, R. P.; Gellman, S. H.; DeGrado, W. F. *Chem. Rev.* **2001**, *101*, 3219−3232. (b) Vasudev, P. G.; Chatterjee, S.; Shamala, N.; Balaram, P. *Chem. Rev.* **2011**, *111*, 657−687.

(4) (a) Appella, D. H.; Christianson, L. A.; Klein, D. A.; Powell, D. R.; Huang, X.; Barchi, J. J., Jr; Gellman, S. H. *Nature* **1997**, *387*, 381−384. (b) Appella, D. H.; Christianson, L. A.; Karle, I. L.; Powell, D. R.; Gellman, S. H. *J. Am. Chem. Soc.* **1999**, *121*, 6206−6212. (c) Appella, D. H.; Christianson, L. A.; Klein, D. A.; Richards, M. R.; Powell, D. R.; Gellman, S. H. *J. Am. Chem. Soc.* **1999**, *121*, 7574−7581. (d) Wang, X.; Espinosa, J. F.; Gellman, S. H. *J. Am. Chem. Soc.* **2000**, *122*, 4821−4822. (e) LePlae, P. R.; Fisk, J. D.; Porter, E. A.; Weisblum, B.; Gellman, S. H. *J. Am. Chem. Soc.* **2002**, *124*, 6820−6821. (f) Izquierdo, S.; Rúa, F.; Sbai, A.; Parella, T.; Álvarez-Larena, Á.; Branchadell, V.; Ortuño, R. M. *J. Org. Chem.* **2005**, *70*, 7963−7971. (g) Fernandes, C.; Faure, S.; Pereira, E.; Théry, V.; Declerck, V.; Guillot, R.; Aitken, D. J. *Org. Lett.* **2010**, *12*, 3606−3609.

(5) (a) Chakraborty, T. K.; Srinivasu, P.; Tapadar, S.; Mohan, B. K. *Glycoconjugate J.* **2005**, *22*, 83−93. (b) Risseeuw, M. D. P.; Overhand, M.; Fleet, G. W. J.; Simone, M. I. *Tetrahedron: Asymmetry* **2007**, *18*, 2001−2010. (c) Risseeuw, M. D. P.; Overhand, M.; Fleet, G. W. J.; Simone, M. I. *Amino Acids* **2013**, *45*, 613−689. (d) Rjabovs, V.; Turks, M. *Tetrahedron* **2013**, *69*, 10693−10710.

(6) (a) Claridge, T. D. W.; Goodman, J. M.; Moreno, A.; Angus, D.; Barker, S. F.; Taillefumier, C.; Watterson, M. P.; Fleet, G. W. J. *Tetrahedron Lett.* **2001**, *42*, 4251−4255. (b) Chandrasekhar, S.; Reddy, M. S.; Jagadeesh, B.; Prabhakar, A.; Rao, M. H. V. R.; Jagannadh, B. *J. Am. Chem. Soc.* **2004**, *126*, 13586−13587. (c) Siriwardena, A.; Pulukuri, K. K.; Kandiyal, P. S.; Roy, S.; Bande, O.; Ghosh, S.; Fernández, J. M. G.; Martin, F. A.; Ghigo, J.-M.; Beloin, C.; Ito, K.; Woods, R. J.; Ampapathi, R. S.; Chakraborty, T. K. *Angew. Chem., Int. Ed.* **2013**, *52*, 10221−10226.

(7) (a) Threlfall, R.; Davies, A.; Howarth, N.; Cosstick, R. *Nucleosides, Nucleotides Nucleic Acids* **2006**, *26*, 611−614. (b) Threlfall, R.; Davies, A.; Howarth, N. M.; Fisher, J.; Cosstick, R. *Chem. Commun.* **2008**, 585−587. (c) Chandrasekhar, S.; Reddy, G. P. K.; Kiran, M. U.; Nagesh, Ch.; Jagadeesh, B. *Tetrahedron Lett.* **2008**, *49*, 2969−2973. (d) Gogoi, K.; Kumar, V. A. *Chem. Commun.* **2008**, 706−708. (e) Bagmare, S.; D'Costa, M.; Kumar, V. A. *Chem. Commun.* **2009**, 6646−6648. (f) Bagmare, S.; Varada, M.; Banerjee, A.; Kumar, V. A. *Tetrahedron* **2013**, *69*, 1210−1216.

(8) Merino, P.; Matute, R. Chemical Synthesis of Conformational Constrained PNA Monomers. In *Chemical Synthesis of Nucleoside Analogues*; Merino, P., Ed.; Wiley-VCH: New Jersey, 2013; pp 847−880.

(9) (a) Egholm, M.; Buchardt, O.; Christensen, L.; Behrens, C.; Freier, S. M.; Driver, D. A.; Berg, R. H.; Kim, S. K.; Norden, B.; Nielsen, P. E. *Nature* **1993**, *365*, 566−568. (b) Nielsen, P. E. *Chem. Biodiversity* **2010**, *7*, 786−804.

(10) (a) Vilaivan, T.; Lowe, G. *J. Am. Chem. Soc.* **2002**, *124*, 9326−9327. (b) Vilaivan, T.; Srisuwannaket, C. *Org. Lett.* **2006**, *8*, 1897−1900. (c) Reenabthue, N.; Boonlua, C.; Vilaivan, C.; Vilaivan, T.; Suparpprom, C. *Bioorg. Med. Chem. Lett.* **2011**, *21*, 6465−6469. (d) Vilaivan, C.; Srisuwannaket, C.; Ananthanawat, C.; Suparpprom, C.; Kawakami, J.; Yamaguchi, Y.; Tanaka, Y.; Vilaivan, T. *Artif. DNA: PNA & XNA* **2011**, *2*, 50−59. (e) Mansawat, W.; Vilaivan, C.; Balázs, Á.; Aitken, D. J.; Vilaivan, T. *Org. Lett.* **2012**, *14*, 1440−1443.

(11) Vilaivan, T. *Acc. Chem. Res.* **2015**, *48*, 1645−1656.

(12) (a) Boontha, B.; Nakkuntod, J.; Hirankarn, N.; Chaumpluk, P.; Vilaivan, T. *Anal. Chem.* **2008**, *80*, 8178−8186. (b) Boonlua, C.; Vilaivan, C.; Wagenknecht, H.-A.; Vilaivan, T. *Chem.—Asian J.* **2011**, *6*, 3251−3259. (c) Laopa, P. S.; Vilaivan, T.; Hoven, V. P. *Analyst* **2013**, *138*, 269−277. (d) Jampasa, S.; Wonsawat, W.; Rodthongkum, N.; Siangproh, W.; Yanatatsaneejit, P.; Vilaivan, T.; Chailapakul, O. *Biosens. Bioelectron.* **2014**, *54*, 428−434.

(13) (a) Pandey, S. K.; Jogdand, G. F.; Oliveira, J. C. A.; Mata, R. A.; Rajamohanan, P. R.; Ramana, C. V. *Chem.—Eur. J.* **2011**, *17*, 12946−12954. (b) Giri, A. G.; Jogdand, G. F.; Rajamohanan, P. R.; Pandey, S. K.; Ramana, C. V. *Eur. J. Org. Chem.* **2012**, 2656−2663.

(14) Sahu, B.; Sacui, I.; Rapireddy, S.; Zanotti, K. J.; Bahal, R.; Armitage, B. A.; Ly, D. H. *J. Org. Chem.* **2011**, *76*, 5614−5627.

(15) Larsen, C. H.; Ridgway, B. H.; Shaw, J. T.; Woerpel, K. A. *J. Am. Chem. Soc.* **1999**, *121*, 12208−12209.

(16) Rabi, J. A. U.S. patent application 2004/0266996 A1, 2004.

(17) (a) Pedersen, C.; Diehl, H. W.; Fletcher, H. G., Jr *J. Am. Chem. Soc.* **1960**, *82*, 3425−3428. (b) Chenault, H. K.; Mandes, R. F. *Tetrahedron* **1997**, *53*, 11033−11038. (c) Adamo, M. F. A.; Adlington, R. M.; Baldwin, J. E.; Day, A. L. *Tetrahedron* **2004**, *60*, 841−849.

(18) Takeshita, M.; Chang, C. N.; Johnson, F.; Will, S.; Grollman, A. P. *J. Biol. Chem.* **1987**, *262*, 10171−10179.

(19) Chong, Y.; Gumina, G.; Mathew, J. S.; Schinazi, R. F.; Chu, C. K. *J. Med. Chem.* **2003**, *46*, 3245−3256.

(20) (a) Dong, H.; Pei, Z.; Ramström, O. *J. Org. Chem.* **2006**, *71*, 3306−3309. (b) Kornblum, N.; Blackwood, R. K.; Mooberry, D. D. *J. Am. Chem. Soc.* **1956**, *78*, 1501−1504. (c) Albert, R.; Dax, K.; Link, R. W.; Stütz, A. E. *Carbohydr. Res.* **1983**, *118*, C5−C6. (d) McGeary, R. P.; Amini, S. R.; Tang, V. W. S.; Toth, I. *J. Org. Chem.* **2004**, *69*, 2727−2730. (e) Dong, H.; Rahm, M.; Thota, N.; Deng, L.; Brinck, T.; Ramström, O. *Org. Biomol. Chem.* **2013**, *11*, 648−653. (f) Ren, B.; Dong, H.; Ramström, O. *Chem.−Asian J.* **2014**, *9*, 1298−1304.

(21) (a) Guo, X.; Liu, C.; Zheng, L.; Jiang, S.; Shen, J. *Synlett* **2010**, 1959−1962. (b) Swamy, K. C. K.; Kumar, N. N. B.; Balaraman, E.; Kumar, K. V. P. P. *Chem. Rev.* **2009**, *109*, 2551−2651.

(22) (a) Tojo, G.; Fernandez, M. TEMPO-mediated Oxidations. In *Oxidation of Primary Alcohols to Carboxylic Acids: A Guide to Current Common Practices*; Tojo, G., Ed.; Springer: New York, 2007; pp 79−103. (b) Dettwiler, J. E.; Lubell, W. D. *J. Org. Chem.* **2003**, *68*, 177−179. (c) Epp, J. B.; Widlanski, T. S. *J. Org. Chem.* **1999**, *64*, 293−295.

(23) (a) Johnson, W. C. CD of Nucleic Acids. In *Circular Dichroism: Principles and Applicaions*; Berova, N., Nakanishi, K., Woody, R. W., Eds.; Wiley-VCH: New York, 2000; pp 703−718. (b) Kang, H.; Chou, P.-J.; Johnson, W. C., Jr; Weller, D.; Huang, S.-B.; Summerton, J. E. *Biopolymers* **1992**, *32*, 1351−1363.

(24) Vorličková, M.; Kejnovská, I.; Bednářová, K.; Renčiuk, D.; Kypr, J. *Chirality* **2012**, *24*, 691−698.

(25) Bergenstråhle, M.; Wohlert, J.; Himmel, M. E.; Brady, J. W. *Carbohydr. Res.* **2010**, *345*, 2060−2066.

(26) Jozwiakowski, M. J.; Connors, K. A. *Carbohydr. Res.* **1985**, *143*, 51−59.

DOI: 10.1021/acs.joc.5b00890
J. Org. Chem. 2015, 80, 7058−7065